A Dual-band Beam-Scanning Reflectarray with Circular Polarization for SatCom millimeter-wave Applications

Aghabeyki, Peyman; Serup, Daniel E.; Zhang, Shuai

Published in:
2024 Asia-Pacific Microwave Conference

DOI (link to publication from Publisher):
10.1109/APMC60911.2024.10867722

Publication date:
2024

Document Version
Accepted author manuscript, peer reviewed version

Citation for published version (APA):
Aghabeyki, P., Serup, D. E., & Zhang, S. (2024). A Dual-band Beam-Scanning Reflectarray with Circular Polarization for SatCom millimeter-wave Applications. In *2024 Asia-Pacific Microwave Conference: Microwaves for Sustainable Future, APMC 2024* (pp. 489-491). IEEE (Institute of Electrical and Electronics Engineers). https://doi.org/10.1109/APMC60911.2024.10867722

A Dual-band Beam-Scanning Reflectarray with Circular Polarization for SatCom millimeter-wave Applications

Peyman Aghabeyki
dept. Electronic Systems
Aalborg University
Aalborg University, Denmark
pag@es.aau.dk

Daniel E. Serup
dept. Electronic Systems
Aalborg University
Aalborg University, Denmark
deserup@es.aau.dk

Shuai Zhang
dept. Electronic Systems
Aalborg University
Aalborg University, Denmark
sz@es.aau.dk

***Abstract*—This study presents a dual-band reflectarray (RA) with circular polarization based on Liquid Crystal (LC) technology. An LC Unit Cell (UC) is proposed which consists of 3 High-Band (HB) elements that are interleaved around a Low-Band (LB) element. The element consists of a cross-patch on top of a slot-loaded square patch. The LC is used as a substrate between the cross and square patch. By applying a variable voltage between the two patches, the resonant frequency of each element changes and provides the required phase difference. A 20×20 element RA is simulated with 400 LB elements and 1200 HB elements. The RA 3-dB gain and Axial Ratio (AR) overlapped bandwidth at 19.5 GHz and 28.5 GHz are 8%, and 9.5%, respectively. The beam-scanning range at each frequency band is ±45º. The proposed design can be a good candidate for the satellite constellations at the millimeter wave.**

Keywords*— *Beam-Scanning, Dual-Band, Circular polarization, Liquid Crystal, Reflectarray, Satcom

I. INTRODUCTION

Reflectarray antennas have proven to be an effective solution to reduce the cost and improve the performance of conventional antenna arrays. It eliminates the lossy RF network for antenna arrays and achieves a high gain with a large number of unit elements. Moreover, in recent years, different types of reconfigurable RAs have been investigated in which varactor Diode [1], PIN diode [2], and mechanical methods [3] are used to achieve beam-scanning. However, in most of the methods, the operating frequency is limited to the Ku band. Recently, PIN diodes have been used in E-band [4]. However, there are several main challenges for PIN diode-based RA fabrication such as PIN diode inaccuracy, large electrical volume of PIN diode, and limited PCB fabrication accuracy. A very promising technology for millimeter wave and subs-terahertz is LC material. LC has several advantages such as limitless operating frequency from X-band to THz, mature and low-cost fabrication technology, and scalability. Different structures based on LC has been proposed such as dual layer patch [5], and aperture coupled Delay Line [6] which uses LC material to provide a phase shift and realize a beam-scanning RA. With the emergence of new Low Earth Orbit (LEO) satellite constellations such as Starlink and OneWeb, higher frequencies are becoming more and more popular to use for this application. For example, in Kuiper and Telesat [7] constellations, down-link and up-link frequency bands are going to be around 19 GHz and 28 GHz, respectively. Therefore, new low-cost beam-scanning antenna technologies at the millimeter wave range with dual-band and circular polarization are very crucial. In this paper, an RA is proposed that operates independently at 19.5 GHz and 28.5 GHz with circular polarization. The simulation results show that the antenna can achieve 8% and 9.5% AR and Gain bandwidth at LB and HB, respectively, and ±45º beam-scanning range.

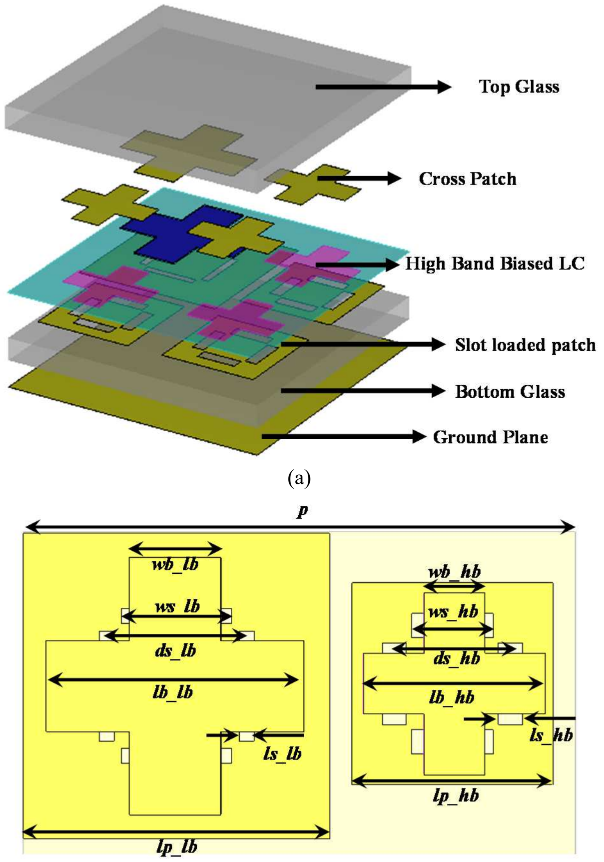

(a)

(b)

Fig. 1. The proposed UC with 3 elements for HB and 1 element for LC. (a) perspective view (b) top via with the design elements. The final design dimensions are *p=5.9 mm, wb_lb =0.954 mm, ws_lb=1.166 mm, ds_lb=1.325 mm, lb_lb=2.7 mm, ls_lb=0.16 mm, lp_lb=1.23mm, wb_hb=0.636 mm, ws_hb=0.836 mm, ds_hb=0.976 mm, lb_hb=1.9 mm, ls_hb=0.257 mm, lp_hb=2.12 mm*

II. UC STRUCTURE

Fig. 1 illustrates the proposed UC for dual-band circular polarization. The detailed operating principle of the UC can be found in [5]. In this work, one large element is used to resonate around 19 GHz which is called Low Band (LB), and three smaller elements are interleaved to resonate around 28.5

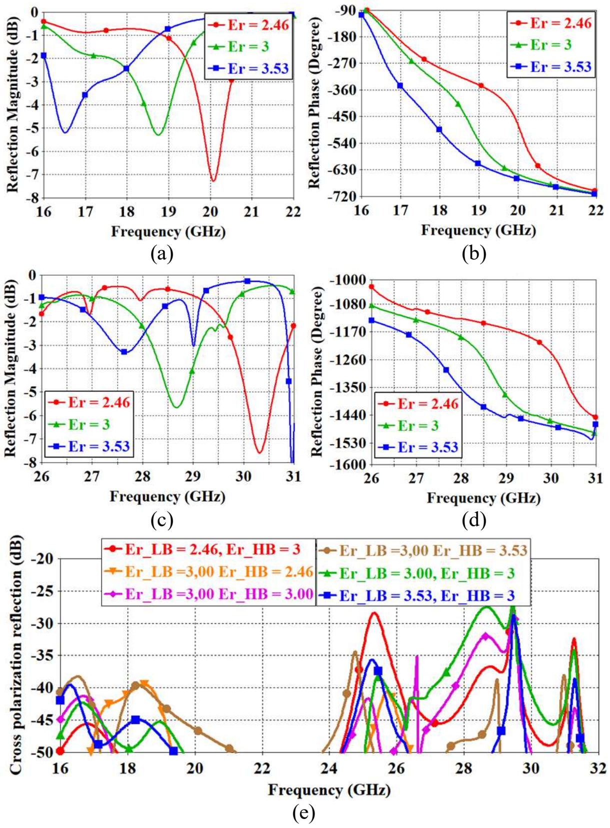

(a) (b)

(c) (d)

(e)

Fig. 2. Reflection coefficient of the UC. (a) LB magnitude, (b) LB phase, (c) HB magnitude and (d) HB phase. (e) The cross-polarization level for both frequency bands.

GHz which is called High Band (HB). The LC is used between the slot-loaded patch and the top cross-patch. By applying a voltage to these two metal layers, an electric field is created in the LC layer and the orientation of LC molecules are changed. This will change the permittivity of the LC material hence, the resonant frequency will change, and the phase shift can be obtained. One drawback of the LC structures is the the response time of permittivity change which is inversely proportional to the thickness of the LC layer. However, with the proposed configuration one can reduce the thickness down to $3.75 \times 10^{-4}\lambda$ and still obtain a good phase shift and loss which helps reduce the response time of the LC-based UC significantly. For this work, the thickness is fixed at 30 µm to compromise between performance and simulation complexity. The glass substrates are 0.5 mm thick Fused Silica with $\varepsilon_r = 3.8$ and $\tan\delta = 0.0002$. For better modeling of the LC, the active area is modeled with a variable permittivity, and the rest is modeled as a constant one. The GT7 LC mixture from Merck Electronics KGaA with $\varepsilon_{r\parallel} = 3.53$, $\tan\delta_{\parallel} = 0.0064$, $\varepsilon_{r\perp} = 2.45$ and $\tan\delta_{\perp} = 0.0117$ is used for the LC layer. To apply the voltage, narrow bias lines with 10 µm width can be printed on the glass and connect the UC elements to the voltage source. The lines can be connected to the junction of the cross patch arms where the electric field is very weak. It should be noted that the bias lines have an insignificant effect on the reflection coefficient and to make the simulation easier, it was not considered in this study. The UC is simulated in Unit Cell boundary conditions with Floquet port excitation and circular polarization in CST Microwave Studio. The reflection coefficient for HB and LB is shown in Fig. 2. The LB has a loss of 7 to 5 dB when the LC permittivity is changed from 2.45 to 3.53 and 265º phase shift can be obtained around 19 GHz. The HB shows 7.5 dB to 3 dB loss with a 290º phase shift in the total permittivity range around 28.5 GHz. The cross polarization level of the entire UC is displayed in Fig. 2 (e) which demonstrates that the structure suppresses the cross-polarization more than -27 dB in the both bands.

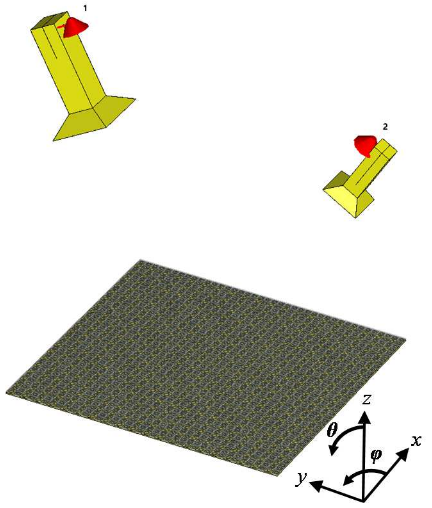

Fig. 3. Simulation setup for dual-band circular polarization reflectarray.

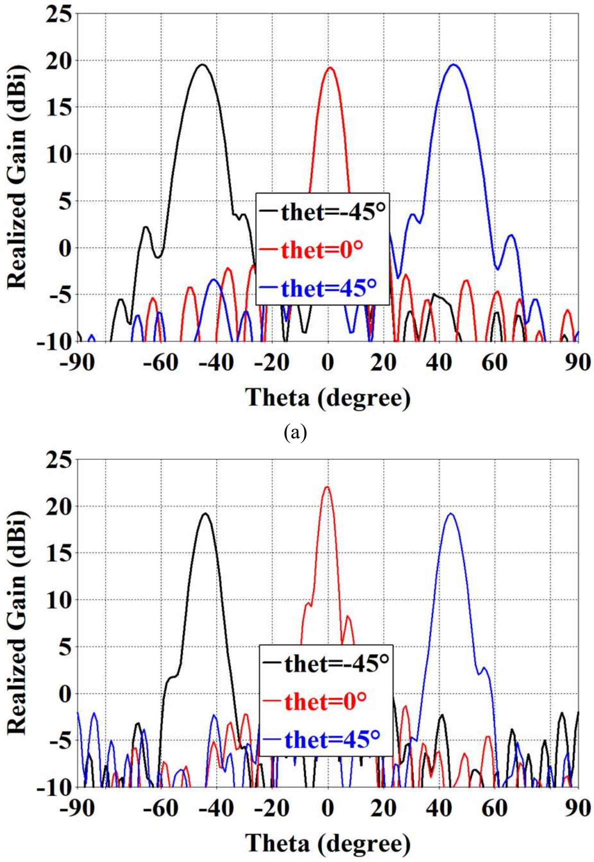

(a)

(b)

Fig. 4. Simulated beam-Scanning radiation pattern for several beam directions in (a) φ = 0º plane of LB at 19.5 GHz and (b) φ = 0º plane of HB at 28.5 GHz.

III. REFLECTARRAY DESIGN

Based on the proposed UC in the previous section, a 20×20 element RA with the size of 118 mm × 118 mm is designed.

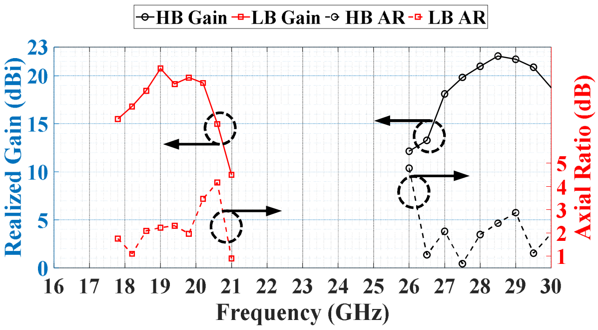

Fig. 5. Simulated maximum gain and AR over frequency for each band at the boresight direction.

The RA surface is illuminated with one circular polarization horn for each band with 11.5 dBi gain. The simulation setup is shown in Fig. 3. The horns are placed at the focal point of z = 95 mm with θ = ±30° tilt in φ = 90° plane. The following expression is used for each element to calculate the phase distribution on the RA surface:

$$\Omega_{mn} = k\times(R_{mn}- \hat{u}_0.r_{mn})+\psi_0 \qquad (1)$$

Where Ω_{mn} is the relative phase of mnth element at each frequency band, k is the wavenumber of the corresponding frequency band in free space, R_{mn} is the distance from the phase center of feed horns to the mnth element, $\hat{u}_0$ is the unit vector of the desired beam direction, r_{mn} is the position vector of the mnth element and ψ_0 is the phase reference. The phase distribution is calculated for several beam directions for each frequency band and the structure is simulated in CST Microwave Studio. The beam steering is displayed in Fig. 4 for center frequency of each band in φ = 0° plane which shows ±45° scanning range in LB and HB. To evaluate the RA performance over frequency, the maximum gain and AR over frequency for boresight direction is depicted in Fig. 5 for each band. It shows that at the LB, the 3-dB realized gain bandwidth is from 18.42 GHz to 20.32 GHz and AR is below 3 dB from 17.24 GHz to 20 GHz which provides 1.6 GHz operating bandwidth. The 3-dB realized gain bandwidth for the HB is from 27.25 GHz to 29.95 GHz and AR is below 3 dB from 26.24 GHz to 30.1 GHz which provides 2.7 GHz operating bandwidth. The results show that the RA can steer the beam at least to ±45° for each band with 8 % AR and Gain bandwidth at 19.5 GHz and 9.5 % AR and Gain bandwidth at 28.5 GHz at boresight. It is worth mentioning that the amplitude and phase response of the UC is not symmetrical around the center frequency and the phase shift cannot cover 360°. Therefore, the phase reference (ψ_0) plays an important role to determine the gain bandwidth and maximum value. The reason behind this is that for each value of ψ_0, the arrangement and total number of dielectric value distribution is different and thus the average loss of the total elements would be different. To have the maximum gain over the desired instantaneous bandwidth, an optimization needs to be done to obtain the best value of ψ_0 at each band. Here, the results are obtained for $\psi_0 = 0$.

IV. CONCLUSION

In this study, a liquid crystal-based UC is proposed with dual band and circular polarization by interleaving one element of the low frequency band among three elements of higher frequency band. The proposed structure possesses a thin LC layer which help improving the response time and beam-scanning speed. The 20 × 20 RA is designed and simulated to validate the performance of the UC. The results show that the RA can steer the beam at least to ±45° for each band with 8 % bandwidth at the LB and 9.5 % bandwidth at the HB.

REFERENCES

[1] E. Baladi, M. Y. Xu, N. Faria, J. Nicholls, and S. V. Hum, "Dual-Band Circularly Polarized Fully Reconfigurable Reflectarray Antenna for Satellite Applications in the Ku Band," *IEEE Trans. Antennas Propag.*, no. c, pp. 1–10, 2021, doi: 10.1109/TAP.2021.3090577.

[2] F. Wu *et al.*, "A 2 bit Circularly Polarized Reconfigurable Reflectarray Using p-i-n-Diode-Tuned Crossed-Bowtie Patch Elements," *IEEE Trans. Antennas Propag.*, vol. 71, no. 9, pp. 7299–7309, 2023, doi: 10.1109/TAP.2023.3291773.

[3] Z. Cao, Y. Li, Z. Zhang, and M. F. Iskander, "Single Motor-Controlled Mechanically Reconfigurable Reflectarray," *IEEE Trans. Antennas Propag.*, vol. 71, no. 1, pp. 190–199, 2023, doi: 10.1109/TAP.2022.3221036.

[4] C. Liu, F. Yang, S. Xu, and M. Li, "An E-Band Reconfigurable Reflectarray Antenna Using p-i-n Diodes for Millimeter-Wave Communications," *IEEE Trans. Antennas Propag.*, vol. 71, no. 8, pp. 6924–6929, 2023, doi: 10.1109/TAP.2023.3291087.

[5] P. Aghabeyki, Y. Cai, G. Deng, Z. H. Tan, and S. Zhang, "A Dual-Polarized Reconfigurable Reflectarray With a Thin Liquid Crystal Layer and 2-D Beam Scanning," *IEEE Trans. Antennas Propag.*, vol. 71, no. 4, pp. 3282–3293, 2023, doi: 10.1109/TAP.2023.3240853.

[6] P. Aghabeyki, Z. Tan, and S. Zhang, "A Wideband Reconfigurable Reflectarray based on Aperture Coupled Delay Line," *2023 17th Eur. Conf. Antennas Propag.*, pp. 1–5, doi: 10.23919/EuCAP57121.2023.10133638.

[7] G. Amendola *et al.*, "Low-Earth Orbit User Segment in the Ku and Ka-Band: An Overview of Antennas and RF Front-End Technologies," *IEEE Microw. Mag.*, vol. 24, no. 2, pp. 32–48, 2023, doi: 10.1109/MMM.2022.3217961.